Digital-sampling systems in high-resolution and wide dynamic-range energy measurements: Comparison with peak sensing ADCs

Luigi Bardelli*, Giacomo Poggi, (NUCL-EX collaboration)

I.N.F.N. and Department of Physics, University of Florence, Via G. Sansone 1, Sesto Fiorentino 50019, Italy

Abstract

The use of fast digital sampling techniques in Nuclear Physics experiments as a replacement of the standard analog signal processing methods is discussed for applications needing high-resolution signal amplitude measurements. This is for example the case of a solid-state detector with a charge-sensitive preamplifier, processed using fast digital sampling methods. Under very general assumptions, an expression for the achievable resolution and dynamic range of the system is reported, valid for any detector/digitizer/digital-filter combination, taking into account the detector noise and the ADC properties, namely the Effective Number of Bits (ENOB) and the sampling frequency. The system properties are summarized using the parameter PSENOB, i.e. the "Peak-Sensing-Equivalent Number of Bits". These results can be used to predict the attainable performances in various applications, possibly requiring a resolution/dynamic-range trade-off. Numerical examples for some representative cases in γ-ray spectroscopy and charged particle experiments are reported, demonstrating that the equivalent performances of a 15 bit peak-sensing ADC are feasible with today-available sampling ADCs. For ease of presentation, other non-trivial effects as baseline- and non-linearity-related issues as well as experimental tests of the proposed approach are presented in a companion paper [L. Bardelli, G. Poggi, Digital sampling-systems in high-resolution and wide dynamic-range energy measurements: finite time window, baseline effects, and experimental tests, this issue].
© 2006 Elsevier B.V. All rights reserved.

1. Introduction

For many Nuclear Physics applications high-resolution amplitude (i.e. energy) measurements of the output of a detector are of paramount importance, as for example in γ spectroscopy measurements or in charged particle detection/identification.

In experiments and proposals where hundreds of detectors are used (for example [2–4]), the standard analog signal processing methods are often replaced by digital sampling systems. The output of the preamplifier (usually a charge-sensitive one) is directly fed into a fast digitizer that produces many sampled points for each detector signal. This data stream is numerically processed with a digital shaping filter in order to improve the signal-to-noise ratio (SNR) and to obtain the desired high-resolution amplitude measurement. Using dedicated hardware, the computation can be performed in real-time, thus realizing a digital spectrometer system.

The properties of the used Analog to Digital Converter (ADC) play a significant role to maintain the intrinsic detector amplitude resolution over a wide dynamic range. For this purpose, the two key parameters are the ADC Effective Number of Bits (ENOB) and its sampling frequency. An increased dynamic range can be obviously achieved using an ADC having a higher resolution, although this usually comes at the expense of a significantly lower sampling rate. This choice is thus not feasible for many applications where energy measurement is not the only parameter of interest. For example in spectroscopy experiments like [3,4], where large volume germanium

*Corresponding author. Tel.: +39 055 4572693.
E-mail address: bardelli@fi.infn.it (L. Bardelli).

detectors are used, an analysis of the pulse shape of the signal is needed in order to reconstruct the γ interaction point. As a further example, in charged particle experiments time coincidences and time of flight measurements are often required, and moreover an analysis of the signal pulse shape is needed in order to identify charge and mass of the detected particles (some experimental results obtained with digital sampling methods are reported for example in Refs. [5–10]). Sampling frequencies in the 50–200 MSamples/s range are needed in order to satisfy most of the experimental needs. For example in Ref. [8], where a 10.8 effective bits, 100 MSamples/s converter is used, a timing resolution of 100 ps FWHM using a silicon detector is presented and discussed. The same system provides a 1.9 ns FWHM resolution at 1.3 MeV with a 30% efficiency germanium detector [10]. From the experimental point of view the possibility of performing energy, timing, and pulse-shape related measurements with a *single* AD converter coupled to the preamplifier is obviously very attractive, and thus a detailed understanding of the relative importance of the ADC ENOB and of the sampling frequency is needed.

Although it is well known in the literature that the availability of many sampled points for each event allows for a kind of "bit-gain" effect [11] (i.e. the finally achievable resolution and dynamic range of a *B*-bits ADC is higher than naïvely expected for the nominal *B* value), this issue has been quantitatively addressed only in a few special cases (see for example Ref. [12]). In this paper a quantitative expression for the contribution to the achievable resolution and dynamic range due to the used fast AD converter and digital filter is proposed, under very general assumptions regarding the various system properties. The relevant ADC and experimental parameters are considered and summarized using the quantity PSENOB (Peak-Sensing-Equivalent Number of Bits). The results are also presented in a plot that can be used as a recipe for simply determining the overall system performances (in terms of energy resolution and dynamic range) in any given experimental condition.

In Section 2 the concept of ADC ENOB is recalled and discussed in view of energy measurement applications, whereas in Section 3 the computation of the achievable performances is carried out under very general hypotheses. In Section 4 the results are discussed and applied to representative examples in the field of Nuclear Physics.

In order to keep the presented discussion as clear as possible, the inclusion of important effects—present in Nuclear Physics experiments—requiring an elaborate discussion (like the use of a finite number of samples and a non-zero baseline) are explicitly addressed in a companion paper [1], where a general expression for the final resolution is given. In Ref. [1] it is also demonstrated that these experimental effects can be kept sufficiently small so that the conclusions of the present paper are not altered. In the same work, the results have been verified with

experimental tests on a germanium detector as well as on $\Delta E - E$ charged particle identification.

The reported discussion and results can be directly extended to various experimental arrangements.

2. Effective Number of Bits for energy measurement applications

Besides the sampling rate f_S, a fast sampling ADC is characterized by its resolution, i.e. the number of bits. An input signal fed into an ADC having B "physical" bits is quantized into 2^B levels.

In the case of a noiseless constant input signal an ideal AD converter should produce a constant conversion code. This is not the case of real ADCs, that output a digital data stream with values fluctuating around the nominal conversion code. The amount of this fluctuation can be quantified with the ENOB (in general a non-integer quantity). Typical values for high-speed ADCs are 1–2 bits below the "physical" number of bits B (for example a 12 bit converter usually has 10–11 effective bits). More technical definitions as well as useful conversion formulæ regarding the ADC SNR, ENOBs, and related quantities, are given in Ref. [13].

The ENOB of an ADC is usually extracted from the SNR obtained from a measurement of a fixed frequency sinusoidal input signal [13,14]. This definition provides an ENOB value that depends on the test frequency and includes various ADC parameters, i.e. thermal noise, non-linearities, aperture- and clock-jitter (see also Ref. [14]). In particular, aperture- and clock-jitter effects give a contribution that is proportional to the derivative of the input signal. Whereas this is the proper definition for applications dealing with fast periodic signals (for example in RF or telecommunication applications), not all these parameters are important for the purpose of amplitude measurements with Nuclear Physics detectors.

A charge preamplifier signal is normally characterized by a preceding nearly constant baseline value, a fast rise and a subsequent much slower decay. The ADC-related noise is thus clearly influenced by ADC thermal noise and non-linearity effects, whereas aperture- and clock-jitter give negligible contributions, as it will be quantitatively shown later (see Appendix A). Accordingly, in the following discussions as well as in the examples of Section 4 the used ENOB value of ADCs does not include jitter effects, i.e. it always corresponds to the value declared by the manufacturer at low frequency. Under these hypotheses, the effect of the sampling process on the overall system noise can be schematized as an additional white-noise source with no correlation with the input signal [15]. The ADC noise variance is given by

$$\sigma_{\text{ADC}}^2 = \frac{R^2}{12} \frac{1}{4^{\text{ENOB}}} = \frac{R^2}{12} \left[\sigma_n^2 + \frac{1}{4^B} \right] \qquad (1)$$

where R is the AD converter range in the used configuration, B the number of "physical" bits (i.e. the quantization

level), and the term σ_n^2 summarizes additional noise sources (like thermal noise and differential non-linearity).[1] The spectral noise density of the converter noise is then given by

$$b_{ADC}(\omega) = \sigma_{ADC}^2 \times \frac{2}{f_S} \quad \text{for } \omega < \frac{f_S}{\pi}. \tag{2}$$

In the following, the total ADC noise contribution will be denoted by "sampling noise".

In other Nuclear Physics applications, time-jitter effects cannot a priori be neglected, for instance when sampling ADCs are used with current-sensitive preamplifiers in amplitude measurements or when used in pulse-shape and timing applications (as for example in Refs. [8,10]). Assuming the worst case of no correlation between the time fluctuations at different samples, the sampling (with jitter) of a continuous signal $p(t)$ with a sampling period τ_{clk} gives a sampled sequence $p[k] = p(\tau_{clk}k + \delta t_{ji})$, where δt_{ji} is a zero-mean random variable with variance σ_{ji}^2. This corresponds to a jitter-related noise $n_{ji}[k] = p'[k] \cdot \delta t_{ji}[k]$, where $p'[k]$ is the derivative of $p[k]$. This noise component is thus non-stationary. The resulting term (see Eq. (A.1)) must then be added to σ_{ADC}^2 of Eq. (1) when jitter-related effects need to be considered.

3. Digital system performances and Peak-Sensing-Equivalent Number of Bits

A signal amplitude (for example energy) measurement as typically performed in Nuclear Physics experiments can be schematized as follows. The determination of the desired quantity E (for example the particle energy) is obtained by the analysis of the output signal $S(t)$ of a detection device. The resulting signal is digitized and shaped with a digital filter in order to improve the SNR. As an example, in typical experiments solid-state/scintillation detectors are used, connected to charge- or current-sensitive preamplifiers/photomultipliers. In the following, with the term "detector" we generally refer to the complete detection system, i.e. including the preamplifier, if present.

If the noisy detector signal is characterized by a (possibly non-constant) shape $p(t)$ and an amplitude proportional to E, the signal $S(t)$ can be written as

$$S(t) = E \cdot p(t) + n(t) \tag{3}$$

where $n(t)$ is the detector electronic noise. We assume that $n(t)$ is described as a stationary random process with zero mean[2] and no correlation with the signal $p(t)$. The spectral noise density of $n(t)$ can be written as

$$w(\omega) = W_a(\omega) + b \tag{4}$$

where b is the white noise component of $n(t)$, and the remaining (non-white) components are summarized in the generic term $W_a(\omega)$. We further suppose that $p(t)$ is a band-limited signal, i.e. no signal components are present for frequencies greater than some value f_N. The shapes $p(t)$ are supposed to be normalized (for example $\max(p) = 1$ for charge-preamplifier-like signals, or $\int p(t)\,dt = 1$ for current-preamplifier-like ones). We define the (ensemble) average signal shape as $\hat{p}(t)$. We further define any resolution worsening on the E measurement due to detection-mechanism properties with σ_D^2, a representative case being statistical fluctuations in the detection process.

As previously discussed, the signal $S(t)$ is fed into a sampling ADC and acquired. The ADC is assumed to have a sampling frequency f_S higher than $2f_N$ (i.e. a perfect reconstruction of $p(t)$ is possible, see [15]) and a proper antialiasing filter cutting at $f_S/2$ (i.e. no over-Nyquist noise components are sampled). This hypothesis allows for seamlessly switching from the discrete to the continuous time domain and viceversa. The following notation will be used—a continuous time quantity, for example $q(t)$, has the discrete-time equivalent $q[k]$, where k is an integer and $t = k\tau_{clk}$.

It has to be noted that all the aforementioned hypotheses can be easily met in ordinary experimental conditions.

A generic linear filter is defined by its response $G(t)$ to a δ-like impulse, hence the dimensions of $G(t)$ are [1/time]. We assume that the digital system has been applying the filter $G(t)$ to the input data since a very long time, i.e. an infinite number of samples is available for processing. The experimentally important case of a finite number of available samples, also in presence of a non-zero baseline, is the main topic of the companion paper [1]. With this notation, the output $R(t)$ of a digital time-invariant filter is given by the convolution between the digitized signal $S(t)$ and $G(t)$.[3] The desired measure $\hat{E}$ of E is obtained by evaluating $R(t)$ at a defined time T_M (for example the time at which the digitally shaped signal reaches its maximum). The system resolution is thus defined as the variance of $R(T_M)$. We fix the (arbitrary) amplitude normalization of $G(t)$ with the condition $\int_{-\infty}^{T_M} \hat{p}(\tau)G(T_M - \tau)\,d\tau = 1$, so that $\hat{E} = R(T_M)$.

For a given digital shaping filter G, we define σ_{th} as the theoretically achievable resolution in the chosen experimental condition, i.e. in the ideal situation where no contribution arises from the digitizer system. The quantity σ_{th} obviously depends not only on the detection system, but also on the used digital filter.

Under these hypotheses, the system resolution can be evaluated. Since we are dealing with several non-stationary quantities, the computation is in general performed in the time domain using ensemble averages, except for those

---

[1]Strictly speaking, the value ENOB to be used in Eq. (1) should not include any integral non-linearity effect, i.e. it is slightly different (higher) from the manufacturer declared value at low frequency. Whereas this last value can be safely used as a conservative assumption, in Ref. [1] integral non-linearity related effects are explicitly considered and shown to be usually negligible.

[2]The case of a non-zero mean is directly related to the baseline-subtraction issues described in detail in Ref. [1].

[3]In the following discussion only the case of time-invariant filters will be explicitly considered. Time-variant filters $G(t, t_0)$ (i.e. the response to a δ-like signal occurring at time t_0) can be included by simply replacing in the following expressions $G(T_M - t)$ with $G(t, T_M)$.

terms where only stationary quantities are present. For the detector noise case, the autocorrelation function $\mathscr{R}(\theta)$ of $n[k]$ is obtained from Eq. (4) using the Wiener–Kintchine theorem. For example, in the case of white noise, $\mathscr{R}(\theta) \propto \delta(\theta)$. The $n[k]$-related contribution σ_n^2 to the overall system resolution is then given by ($T_M = \tau_{clk} N_M$):

$$\sigma_n^2 = \sum_{k,h=-\infty}^{N_M} G[N_M - k]G[N_M - h] \cdot \mathbb{E}_t\{n[k]n[h]\}$$

$$= \int\int_{x,y=-\infty}^{T_M} G(T_M - x)G(T_M - y)\mathscr{R}(x - y)\,dx\,dy. \quad (5)$$

Ensemble averages have been replaced by time averages $\mathbb{E}_t\{\}$ due to the adopted stationary hypothesis on $n[k]$, and the second equivalence follows from passing to continuous variables.

The resolution σ_{th} of the E-measurement, i.e. the variance of the quantity $\widehat{E}$, can then be computed and gives

$$\sigma_{th}^2 = H_G^2 + bk_G^2 + \sigma_p^2 + \sigma_D^2 \quad (6)$$

where the term σ_p^2 is related to the shape variations of $p(t)$, σ_n^2 has been split into the non-white- and white-related terms (H_G^2 and bk_G^2, respectively), and k_G is given by

$$(k_G)^2 = \frac{1}{2}\int_{-\infty}^{T_M} [G(T_M - t)]^2\,dt. \quad (7)$$

The quantity k_G includes the characteristics of the filter and it is easily computed for any given filter. k_G is related to the "delta-noise index" $\langle N_\Delta^2 \rangle$ as defined in Ref. [16] by $(k_G)^2 = \frac{1}{2}\langle N_\Delta^2 \rangle$.

We define the quantity $R/3\sigma_{th}$ as the theoretical dynamic range of the system, i.e. we assume $3\sigma_{th}$ as the signal threshold of the system, having R as full range. The value R may be larger than the maximum expected signal amplitude, in order to take in account the possibility of pile-up events (see for example the "rescaling factor" of Ref. [12]).

We now define σ_{exp} as the experimental resolution obtained using the very same digital filter $G(t)$, and taking into account the presence of the sampling noise. As discussed in Section 2 this effect is related to the ADC ENOB. In Appendix A it is shown that the additional ADC jitter-related contribution is negligible with respect to the ENOB one in all practical cases of interest in Nuclear Physics experiments, and thus in the following only the term in Eq. (1) is retained. In this hypothesis, recalling that the sampling process can be schematized as an additional white-noise contribution to $S(t)$, σ_{exp}^2 can be simply computed including b_{ADC} (Eq. (2)) in the white-noise related term of Eq. (6). The ratio between σ_{exp}^2 and σ_{th}^2 is then given by $1 + b_{ADC}k_G^2/\sigma_{th}^2$, which can be written as

$$\frac{\sigma_{exp}^2}{\sigma_{th}^2} = 1 + \frac{9}{12}\left(\frac{R}{3\sigma_{th}}\right)^2 \cdot \frac{1}{4^{PSENOB}} \quad (8)$$

with the definition:

$$PSENOB = ENOB + \frac{1}{2}\log_2\left(\frac{f_S}{k_G^2}\right) - \frac{1}{2}. \quad (9)$$

We name PSENOB as the "Peak-Sensing-Equivalent Number of Bits". As a matter of fact, it is easily recognized that Eq. (8) has the same structure as if a peak-sensing ADC (or an ADC producing only one sample for each signal) were used in a hypothetical analog system employing the filter G. As a consequence, the quantity PSENOB directly gives the number of bits required by a "traditional" peak-sensing ADC to achieve the same performances of the given digital sampling and shaping system in terms of resolution and dynamic range. The term f_S/k_G^2 can be interpreted as the number of points acquired by the digitizer during a "characteristic" time of the filter, as determined by $1/k_G^2$ (see also Section 4).

As a particular case, when no filtering is applied, i.e. the measurement is performed using only one sample at $t = T_M$, one has $G(t) \propto \delta(t)$ and $k_G^2 = f_S/2$, so that PSENOB $\equiv$ ENOB, as expected.

The adopted formalism allows to quantify the "bit-gain" effect that is present in energy measurements performed with digital sampling methods, i.e. an important increase of the system performances due to the availability of many sampled points for each waveform. In the next section it will be shown that, in the special case of energy measurements with solid-state detectors, a "bit-gain" of the order of 3–5 bits is achieved in typical experimental conditions with the today-available fast sampling AD converters.

Since no special assumption on the detector spectral noise density $w(\omega)$, on the (possibly varying) detector signal shape $p(t)$, and on the detector resolution σ_D^2 is required to obtain Eqs. (8) and (9), these equations can be applied to any measurement of an "amplitude"-related quantity E. An extension of Eq. (8) to those cases where a finite time window is available and baseline-related effects are present is reported in Ref. [1], and it maintains the PSENOB definition of Eq. (9).

The predictions of Eq. (8) for various PSENOB values are presented as solid curves in Fig. 1 (bottom panel) as a function of the theoretical dynamic range $R/3\sigma_{th}$. In the upper panel of the figure the attainable dynamic range $R/3\sigma_{exp}$ is shown as percentage of the theoretical $R/3\sigma_{th}$. Examples of application are presented in Section 4.

Fig. 1 can be used as a recipe for determining the overall system performances using a given fast AD converter and any digital filter in various experimental configurations, possibly requiring a resolution/dynamic-range trade-off. In practical applications of Fig. 1, an estimate of σ_{th} can be obtained by performing a resolution test in a very small dynamic-range configuration, using either a state-of-the-art analog system (possibly using a filter as "close" as possible to G) or a sampling digital system implementing $G(t)$.
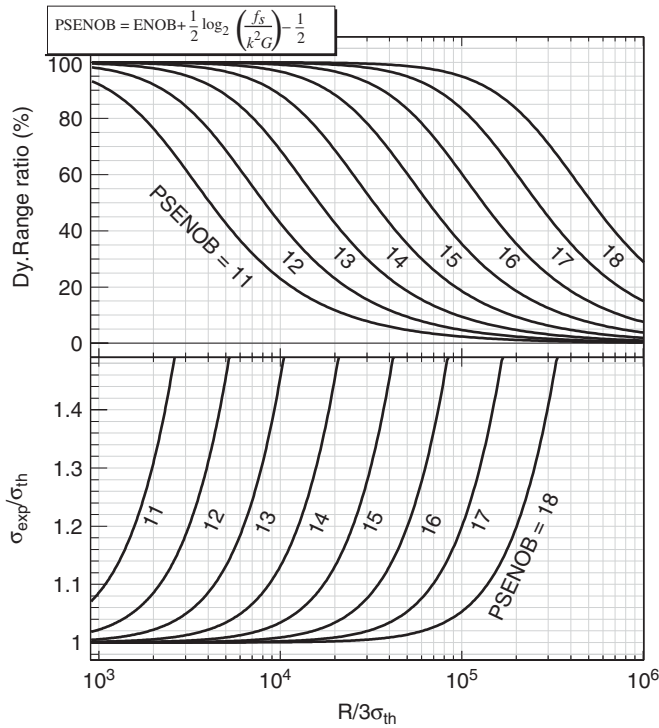
Fig. 1. Predicted experimental resolution (bottom panel) and dynamic range (top panel) obtained from Eq. (8) for various sampling systems, as described by their PSENOB. The curves can be used as a universal guideline to evaluate the overall detector and digital shaping-system performances. See text for details.

In those cases where only electronic resolutions are of concern, the presented results can be applied by simply discarding the terms σ_p^2 and σ_D^2. When detector-and shape-related effects need to be considered it is possible either to directly apply the presented formulas including σ_p^2 and σ_D^2, or to simply add the σ_p^2 and σ_D^2 terms to the computed electronic resolution.

The presented discussion does not include any resolution optimization issue, i.e. the possibility of using different values for the filter parameters in $\sigma_{\exp}$ and σ_{th} in order to take into account (and partially compensate for) the additional ADC noise. An example of this optimization in a particular experimental case is presented in the next section.

4. Applications to energy measurements with solid state detectors

The general approach presented in the previous section is now applied to the representative case of high-resolution energy measurements with solid state detectors (germanium or silicon) connected to charge-sensitive preamplifiers, assuming $p(t)$ as a perfect step signal.

The spectral noise density at the output of the preamplifier is assumed to have the "standard" behaviour $w(\omega) = a/\omega^2 + b$. The noise corner time constant is defined as $\tau_C = \sqrt{b/a}$.

Table 1
The quantity $k_{G\star}$ is reported for various filter types and two choices of the parameter ϑ, i.e. the maximum time T_M and the detector $\tau_{C,opt}$ (see text for details). "Trapezoidal 1" is a trapezoidal filter with a flat top time equal to the linear rise time, whereas in "Trapezoidal 2" the flat top time is half the rise time

Filter	$k_{G\star}$	
	$\vartheta = T_M$	$\vartheta = \tau_{C,opt}$
CR-RC	0.961	0.961
Trapezoidal 1	1.414	0.955
Trapezoidal 2	1.225	0.874
CR-RC[4]	1.012	0.823
Triangular	1.000	0.760
Infinite cusp	–	0.707

Typical filters used in spectroscopy measurements (i.e. triangular, trapezoidal, CR-RC^n) depend on a single shaping time parameter ϑ.[4] These filters can be written as

$$G(t) = \frac{1}{\vartheta} \, G^\star\left(\frac{t}{\vartheta}\right) \tag{10}$$

where the adimensional $G^\star(x)$ represents the filter "shape" and ϑ is used as scaling parameter, whose value is usually chosen in order to adapt the filter to the experimental noise figure. By defining $(k_{G\star})^2 = \frac{1}{2}\int[G^\star(x)]^2 \, dx$, it is easily verified that

$$k_G^2 = \frac{k_{G\star}^2}{\vartheta}. \tag{11}$$

Regardless to the used scaling parameter ϑ, for a given filter $G(t)$ the simple relation $k_{G\star}^2/\vartheta = $ constant holds. In Table 1 the value of $k_{G\star}$ for some representative filters is reported, for two different choices of the (arbitrary) scaling parameter ϑ. In the first column, ϑ is the time T_M at which the shaped signal reaches its maximum if the detector signal starts at $t = 0$ ($T_M \to \infty$ for the infinite cusp). In the second column ϑ is the detector corner time $\tau_{C,opt}$ at which the filter provides its optimal performances when applied to a detector with $a/\omega^2 + b$ noise. This last choice, although not directly related to any filter shape parameter, allows for a simple resolution comparison between the listed filters. Besides, it is easily seen from Eqs. (9) and (11) that, due to the moderate dependence of $k_{G\star}$ from the filter shape (if $\vartheta = \tau_{C,opt}$ in Table 1), the key factor in determining the system "bit gain" is directly related to $f_S\tau_{C,opt}$, i.e. the number of sampled points in the $\tau_{C,opt}$ time span.

Using the listed $k_{G\star}$ values, it is now possible to apply the general results of the previous section to typical experimental Nuclear Physics setups and to evaluate the resulting performances.

For example, by using an 11 ENOB, 100 MSamples/s converter, optimized CR-RC^4 shaping, with a detector/ preamplifier system having $\tau_{C,opt} \simeq 6\,\mu s$ (this configuration

---

[4] We assume that the remaining filter parameters are proportional to ϑ and fixed using other constraints (as for example ballistic deficit compensation).

is similar to the simulated and experimental tests of Ref. [1]), the value PSENOB $\simeq 15$ is obtained, i.e. the performances of this system are expected to be the same as using a $\simeq 15$ bit peak-sensing ADC. If this digitizer is employed in an experimental setup using a germanium detector with a theoretical electronic resolution of about 0.7 keV FWHM and full range $R \simeq 10$ MeV (i.e. operating conditions similar to those of future γ-arrays [3,4]), the value $\sigma_{exp}/\sigma_{th} = 1.04$ is extracted from the figure. This corresponds to a predicted electronic resolution of the overall system of about 0.73 keV FWHM, i.e. within few percents of the theoretically maximum achievable value. This small effect on the electronic resolution has practically no influence on the final resolution when, for example, γ-rays with energies greater than a few hundreds of keV are of interest, due to the added statistical fluctuations (i.e. the term σ_D^2 in Eq. (6)).

As a further example, let us assume to have a silicon/preamplifier system with 60 keV FWHM electronic resolution, $\tau_{C,opt} \simeq 1.9\,\mu s$, and a desired full range $R = 2$ GeV. This situation is similar to the experimental tests presented in Ref. [1] but for a infinite baseline time. The predicted system performances can be obtained from Fig. 1 using a dynamic range of $\sim 2.6 \times 10^4$. The use of a 100 MSamples/s, 11 ENOB converter with an optimal CR-RC^4 shaping provides PSENOB $\simeq 14.4$, i.e. an experimental dynamic range of $\sim 1.8 \times 10^4$. In this example a significant electronic resolution degradation can be tolerated in view of the wide dynamic range aimed at. The apparent reduction of the PSENOB value with respect to the preceding example is immediately traced back to the shorter detector noise corner time, which—as already discussed—significantly reduces the number of samples used for shaping.

Further performance improvement can be achieved recalling that Eq. (8) has been obtained in the hypotheses of using the very same digital filter (i.e. the same value for the parameter ϑ for the kind of filters of Eq. (10)) for both the theoretical and the experimental resolutions. In many applications, it is possible to modify the value of ϑ used in the experiment in order to reduce the importance of the ADC white noise, i.e. by using longer shaping time constants. Performing the calculation, recalling the $a/\omega^2 + b$ noise hypothesis, one obtains:

$$\frac{\sigma_{exp,opt}^2}{\sigma_{th,opt}^2} = \sqrt{1 + 2 \cdot \frac{9}{12}\left(\frac{R}{3\sigma_{th}}\right)^2 \frac{1}{4^{PSENOB}}}. \tag{12}$$

The notation "opt" refers to the use of the optimal filter-parameter. The effect of this further optimization is only negligible for $\sigma_{exp}/\sigma_{th,opt} \sim 1$. For example, in the previous case regarding the silicon detector, the resulting dynamic range after this optimization is about $\sim 1.95 \times 10^4$, i.e. a 10% improvement is obtained. The use of Eq. (12) implies a longer shaping time parameter ϑ with respect to the one used for obtaining $\sigma_{th,opt}$, precisely an increase of the shaping parameter by a factor $\sigma_{exp}^2/\sigma_{th,opt}^2$. Since in an experimental measurement the available range for ϑ is usually limited by several constraints (like counting rate), this further optimization is not always feasible from a practical point of view.

5. Conclusions

In this paper a quantitative evaluation of the performances of fast digital sampling-systems for applications requiring high-resolution and wide dynamic-range energy measurements has been presented. A simple expression of the achievable resolution has been proposed as a function of the dynamic range of the system, valid for any detector/preamplifier/AD converter/digital filter combination. The parameter PSENOB, i.e. the "Peak-Sensing-Equivalent Number of Bits", has been proposed to describe the obtained performances in analogy to "traditional" peak sensing systems, thus allowing for an easy comparison with state-of-the-art analog systems. The computation has been performed under very general assumptions for the various detector properties, and then discussed for some typical cases of Nuclear Physics applications. For example, using the proposed recipe, a typical fast AD converter (10–12 ENOB, 50–200 MSamples/s) is able to reach and overcome the performances of a 15 bit peak-sensing ADC.

A complete replacement of the traditional analog systems is possible given the predicted performances of the presently commercially available sampling ADCs, with the additional bonus of a significant simplification of the experimental setups. In order to fully exploit the performances of these converters a corresponding effort has to be dedicated to improve the dynamic range of detection and preamplification systems, at least in the field of charged particle detection and identification over wide energy, charge, and mass ranges. Clean cabling, differential signal transmission, and proper triggering of the system are also needed in order to exploit the achievable dynamic range.

While not considered in this paper, in the companion paper [1] experimentally important issues like the use of a finite number of samples for digital shaping and the presence of a non-zero baseline level are quantitatively addressed and extended prescriptions are provided for the final energy resolution. As a matter of fact, in Ref. [1] it is shown that in practical applications it is possible to reduce the importance of both the aforementioned effects, so that the conclusions of the present paper are not altered. Experimental tests validating this presentation are presented in the companion paper [1].

Appendix A. Evaluation of time-jitter effects

In this Appendix the evaluation of time-jitter related effects is carried out. As it will be shown, these effects can usually be neglected in typical Nuclear Physics applications.

Using the definitions given in Section 2, recalling the worst case hypothesis of uncorrelated $\delta t_{ji}[h]$, and carrying out the computation in the finite-time domain, the non-stationary jitter-related effect on σ_{exp} is given by an additional σ^2 term:

$$\sigma^2 = E^2 \sigma_{ji}^2 \frac{k_{ji}^2}{f_S} \tag{A.1}$$

where k_{ji} is given by

$$(k_{ji})^2 = \int_{-\infty}^{T_M} [p'(t) G(T_M - t)]^2 \, dt. \tag{A.2}$$

The dimensions of $(k_{ji})^2$ are thus [1/time³]. Comparing Eq. (A.1) with the ENOB-related one (i.e. $b_{ADC} k_G^2$), it is easily verified that the jitter term is negligible if the following holds:

$$\sigma_{ji}^2 \ll \frac{2}{12} \frac{1}{4^{ENOB}} \frac{R^2}{E^2} \frac{k_G^2}{k_{ji}^2}. \tag{A.3}$$

Using these results one can extend the given PSENOB definition as

$$\text{PSENOB} = \text{ENOB} + \frac{1}{2} \log_2\left(\frac{f_S}{k_G^2 + 6\sigma_{ji}^2 k_{ji}^2 4^{ENOB}}\right) - \frac{1}{2}. \tag{A.4}$$

In a typical case of interest in Nuclear Physics applications, the signal $p(t)$ is the output of a charge-preamplifier. In this case, the signal portion mainly influenced by the time jitter is the signal risetime that, anyway, does not significantly contribute to the final energy measurement due to its short length compared to a typical shaping time.

To examine this case, let us start by schematizing the signal with a step-like shape. The digitally shaped output is therefore simply given by $\int G(t) \, dt$. The derivative $p'(t)$ is $p'(t) \propto f_S \delta(t)$. Substituting into Eq. (A.2), and taking into account that the measuring point T_M is typically chosen as the time where the shaped signal reaches its maximum, i.e. in the "flat-top" area where $G(t) = 0$, one obtains $k_{ji}^2 = 0$ and thus, in this approximation, zero jitter effects.

More realistic cases can be easily considered by an exact evaluation of Eq. (A.3). For example, we consider a trapezoidal filter with rise-time 3 μs, flat top time 1 μs, and compensated for the signal decay time. The evaluation of Eq. (A.3) shows that an 11 ENOB converter sampling a charge-preamplifier signal with a 100 ns/50 μs rise/decay time combination provides $\sigma_{ji} \ll 2400$ ps (1700 ps for 50 ns/50 μs, 320 ps for 100 ns/5 μs). When the same system is used to sample a current-preamplifier or photomultiplier signal having 10 ns rise time, 30 ns fall time we obtain $\sigma_{ji} \ll 30$ ps. In common operating conditions these limits are easily met using commercially available ADCs (typical aperture jitter 0.1–1 ps) and quartz oscillators (typical jitter 1–4 ps).

In all the examined cases any time-jitter effect is thus negligible.

References

[1] L. Bardelli, G. Poggi, Digital sampling-systems in high-resolution and wide dynamic-range energy measurements: finite time window, baseline effects, and experimental tests, this issue.

[2] Final report of the EURISOL project (European Isotope Separation On-Line Radioactive Ion Beam Facility), available on http://www.ganil.fr/eurisol/Final_Report.html

[3] Technical proposal for the Advanced GAmma Tracking Array (AGATA) project, available on http://agata.pd.infn.it/

[4] M.A. Deleplanque, et al., Nucl. Instr. and Meth. A 430 (1999) 292.

[5] L. Bardelli, et al., Nucl. Instr. and Meth. A 491 (2002) 244.

[6] L. Bardelli, et al., Application of a fast digital sampling system to $\Delta E - E$ identification and subnanosecond timing, Laboratori Nazionali di Legnaro Annual Report, 2002.

[7] L. Bardelli, et al., Proceedings of RNB6 Conference, 2003, Nucl. Phys. A 746 (2004) 272.

[8] L. Bardelli, et al., Nucl. Instr. and Meth. A 521 (2004) 480.

[9] L. Bardelli, et al., Proceedings of the IWM2003 Workshop, 5–7 November 2003, Ganil, France, available on http://www.ganil.fr/iwm2003

[10] L. Bardelli, et al., in: G. La Rana, C. Signorini, S. Shimoura (Eds.), Proceedings of the Fifth Italy–Japan Meeting, 3–7 November 2004, Naples, Italy, World Scientific 2006, ISBN-981-256-523-X.

[11] A. Pullia, A. Geraci, G. Ripamonti, Nucl. Instr. and Meth. A 439 (2000) 378.

[12] A. Georgiev, W. Gast, IEEE Trans. Nucl. Sci. NS-40 (4) (1993) 770.

[13] Analog Devices, Fundamentals of sampled data systems, Application note AN-282.

[14] Analog Devices, Aperture uncertainty and ADC system performance, Application note AN-501.

[15] A.V. Oppenheim, R.W. Shafer, Digital Signal Processing, Prentice-Hall, Englewood Cliffs, 1975.

[16] F.S. Goulding, Nucl. Instr. and Meth. 100 (1972) 493.